Submission code: VALGRWM0X0

See this and other abstracts on our website: https://home.sbgf.org.br/Pages/resumos.php

Limitations of Isotropic NMO Correction in the Presence of Anisotropy

Ana Paula Silva (GISIS/UFF), Felipe Costa (GISIS/UFF), Rodrigo Stern (GISIS/UFF), Marco Cetale (GISIS/UFF)

Limitations of Isotropic NMO Correction in the Presence of Anisotropy

Copyright 2025, SBGf - Sociedade Brasileira de Geofísica / Society of Exploration Geophysicist.
This paper was prepared for presentation during the 19th International Congress of the Brazilian Geophysical Society held in Rio de Janeiro, Brazil, 18-20 November 2025. Contents of this paper were reviewed by the Technical Committee of the 19th International Congress of the Brazilian Geophysical Society and do not necessarily represent any position of the SBGf, its officers or members. Electronic reproduction or storage of any part of this paper for commercial purposes without the written consent of the Brazilian Geophysical Society is prohibited.

Abstract Summary

This study evaluates the impact of applying the Normal Moveout (NMO) isotropic correction to synthetic 2D seismic data in the presence of anisotropy. Two data sets were generated using a simple stratigraphic model: one isotropic and the other incorporating VTI anisotropy in a shale layer. After performing the isotropic velocity analysis and applying the NMO correction to both datasets, a reduction in event alignment and stacking quality was observed in the anisotropic data. These results demonstrate the risks of ignoring anisotropy in processing workflows.

Introduction

Vertical Transverse Isotropy (VTI) seismic anisotropy is a common feature in layered shales, where the elastic properties vary with the direction of wave propagation (Sondergeld, 2011; Thomsen, 1986). Assuming isotropy during seismic data processing can result in significant distortions, such as shifts in arrival times, incorrect event curvatures, and losses of resolution in stacking. This work investigates the impact of anisotropy on seismic data by comparing two synthetic datasets: one generated from an entirely isotropic model and the other that includes VTI anisotropy in one of its layers. Both datasets were processed using velocity analysis and isotropic NMO correction. The objective is to demonstrate how ignoring anisotropy during processing can affect the quality of the seismic image.

Method

We generate isotropic and anisotropic elastic seismic data using a simple stratigraphic model composed of four plane-parallel layers. These layers represent conditions typically associated with water, shale, sandstone, and halite. The first model assumed all layers to be isotropic, and the second incorporated VTI anisotropy exclusively in the shale layer, with Thomsen parameters defined as ϵ = 0.2; δ = 0.2.

The model was originally defined using elastic properties (v_p, v_s and ρ) based on values from da Silva (2022). The v_p values assigned to the four layers were 1500 m/s, 2800 m/s, 3400 m/s, and 4500 m/s. However, despite using the elastic wave equation for the simulations, acoustic parameters were adopted by setting $v_s = 0$ and ρ = 1000 kg/m^3 uniformly in all layers. Figure 1 presents snapshots of wave propagation for the two simulated cases, highlighting differences in wavefront behavior between the isotropic and anisotropic models.

Seismic wave propagation was modeled using the stress-velocity formulation of the elastic wave equation Virieux (1986), discretized on a standard staggered grid in the time domain:

$$\begin{cases} \rho\,\partial_t v_i - \partial_j \sigma_{ij} = f_i, \\ \partial_t \sigma_{ij} - C_{ijkl}\partial_l v_k = -\partial_t g_{ij}, \end{cases} \tag{1}$$

where ρ is the density, v_i is the particle velocity, σ_{ij} is the stress tensor, C_{ijkl} is the stiffness tensor, f_i represents body forces, and g_{ij} accounts for stress sources. The indices i,j,k, and l represent the directions x and z.

Isotropic and anisotropic properties are incorporated into the seismic modeling via the stiffness tensor. For 2D vertical transverse isotropy (VTI), the stiffness matrix in Voigt notation is defined as Tsvankin (2012):

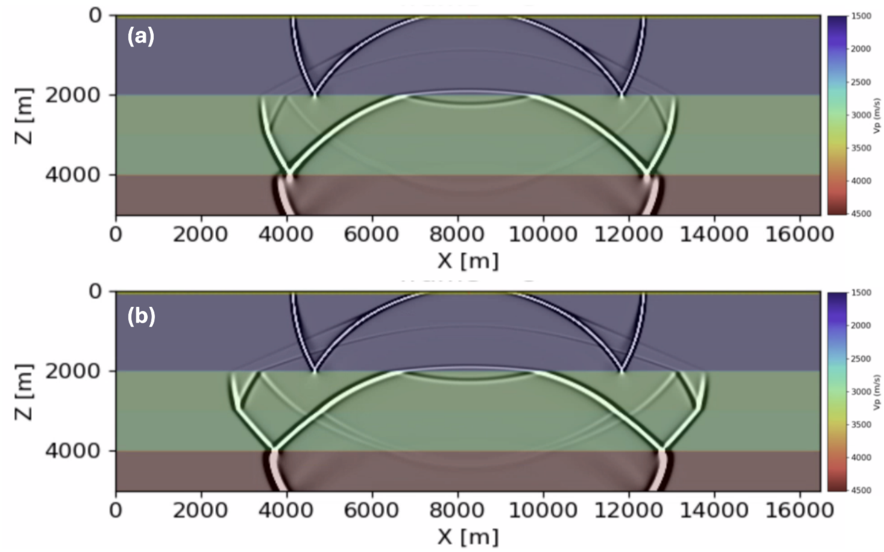

Figure 1: Snapshots of wave propagation for the two simulated cases, overlaid on the v_p model. Figure (a) shows the snapshot for the isotropic case, and (b) corresponds to the VTI anisotropic case.

$$C_{IJ} = \begin{bmatrix} C_{11} & C_{13} & 0 \\ C_{13} & C_{33} & 0 \\ 0 & 0 & C_{55} \end{bmatrix}, \tag{2}$$

with the components given by:

$$C_{11} = \rho v_p^2(2\epsilon + 1) = (\lambda + 2\mu)(2\epsilon + 1) \tag{3}$$

$$C_{33} = \rho v_p^2 = (\lambda + 2\mu) \tag{4}$$

$$C_{55} = \rho v_s^2 = \mu \tag{5}$$

$$C_{13} = \sqrt{2\delta C_{33}(C_{33} - C_{55}) + (C_{33} - C_{55})^2} - C_{55}, \tag{6}$$

The isotropic case is recovered when $\epsilon = 0$ and $\delta = 0$.

Both simulations were performed on acoustic property models measuring 16.4 km in length and 5 km in depth, discretized using a grid with 10 m horizontal and 10 m vertical spacing. The simulations used a time step of 0.5 ms and a total duration of 6 seconds. The acquisition geometry followed an end-on configuration, with 163 sources spaced every 50 m at a depth of 5 m, and 796 receivers spaced every 10 m at a depth of 10 m, covering offsets from 150 m to 8100 m.

Both datasets were organized into CDP gathers and subjected to isotropic velocity analysis using conventional semblance with parameters adjusted for the model's offset and frequency ranges. From the resulting V_{NMO} curves, isotropic NMO correction and common stacking were applied to both models. The results were evaluated through visual inspection of CDP gathers before and after correction and the stacked sections.

Results

The analyses indicate important differences in the behavior of the data after applying the isotropic NMO correction. Although the CMP gathers (Figure 2) of the two data sets show reasonable alignment for the short offsets, in the larger offsets of the VTI data, it is observed that the reflectors are still curved, indicating the presence of moveout residues. This effect, known as “hockey sticks”, is related to anisotropy, which has not been fully corrected by isotropic NMO and also influences the deeper layers. In the reflector related to Layer 3, these effects become even more evident, with sharper residual curvatures in the reflectors, indicating an accumulation of errors in the correction as the depth increases.

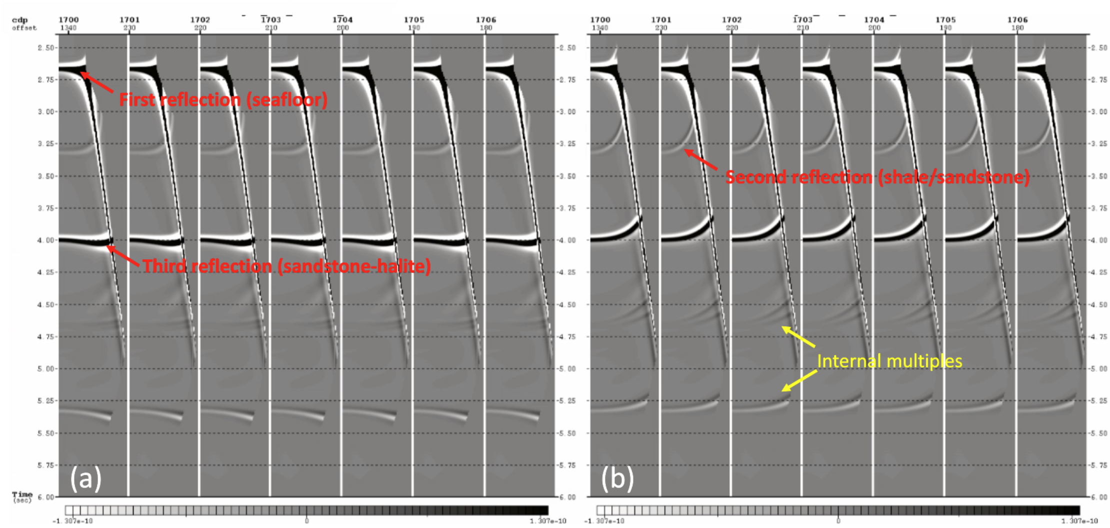

Figure 2: CMP gathers after isotropic NMO correction: (a) isotropic data and (b) VTI data. Pointing out the differences in moveout and reflector curvature between the two cases.

In the stacked sections (Figure 3), the differences become more evident. The stacking of the isotropic model shows well-defined reflectors, while the VTI model exhibits localized distortions, mainly in intervals corresponding to Layer 2.

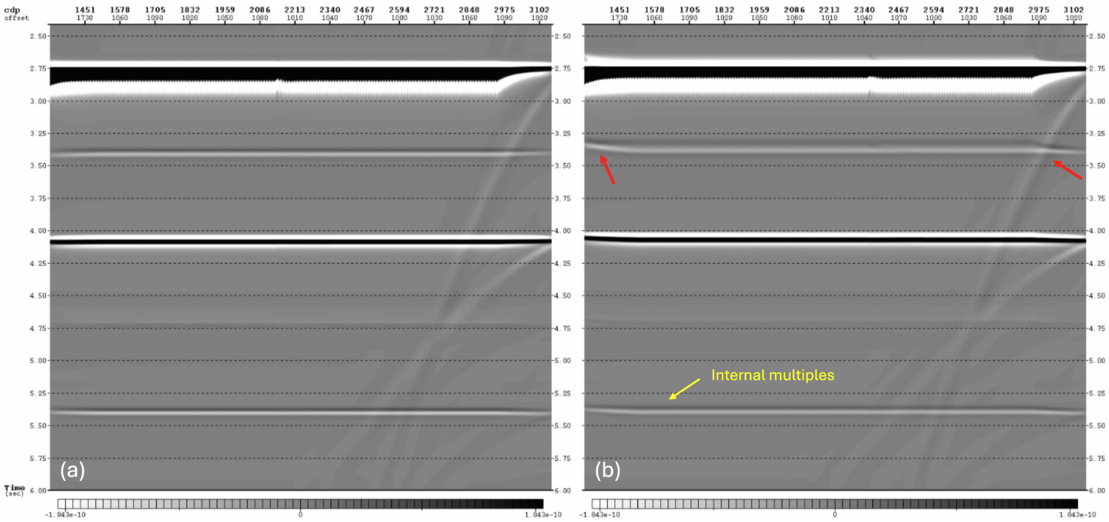

Figure 3: Stacked sections after isotropic NMO correction: (a) isotropic case and (b) VTI case. Differences in the continuity and curvature of the reflector between the two cases are marked with red arrows.

The reflections highlighted in yellow in the CDP gather (Figure 2) correspond to multiple internal and edge effects resulting from the modeling. Although they are present in the data, these reflections do not compromise the analysis. In the 2D stack, they appear as an artifact just below the third reflection, but, as in the gather, they do not affect the interpretation.

Conclusions

The analysis of the datasets shows that applying isotropic processing to anisotropic data results in distortions in the seismic image. In the VTI model, the application of isotropic NMO correction resulted in residual moveout in the CDP gathers, initially in Layer 2, but propagating to the subsequent layers. These results demonstrate the cumulative impact of anisotropy on wave propagation, showing that, even in synthetic and controlled scenarios, the consideration of anisotropy is essential for correct velocity analysis and more accurate seismic images.

As future work, it is proposed to estimate the anisotropic parameters directly from the modeled data and to apply depth migration using anisotropic velocity models in order to assess the imaging errors resulting from incorrect velocity assumptions.

Acknowledgments

The authors from Fluminense Federal University acknowledge the financial support from Petrobras through the R&D project *Modelagem Visco-Elástica Anisotrópica em dados Multi-Azimutais para Análise de Sensibilidade de Sistemas de Fraturas* (ANP nº 24643-9). The strategic importance of the R&D levy regulation of the National Agency for Petroleum, Natural Gas and Biofuels (ANP) is gratefully appreciated. The authors would also like to acknowledge AspenTech for providing the academic license for the software suite used in this research. We would like to thank Mr. Rodrigo Stern (GISIS/UFF) for the IT support.

References

da Silva, G. H., 2022, Anisotropia em meios intercalados e efetivos análises cinemática e de amplitudes: PhD thesis, Universidade Federal Fluminense.

Sondergeld, C. H., 2011, Elastic anisotropy of shales: The Leading Edge.

Thomsen, L., 1986, Weak elastic anisotropy: GEOPHYSICS, **51**, no. 10, 1954–1966.

Tsvankin, I., 2012, Seismic signatures and analysis of reflection data in anisotropic media: Society of Exploration Geophysicists.

Virieux, J., 1986, P-SV wave propagation in heterogeneous media: Velocity-stress finite-difference method: Geophysics, **51**, 889–901.